

Vessel tractography using an intensity based tensor model

Suheyla Cetin¹, Gozde Unal¹, Ali Demir¹, Anthony Joseph Yezzi², and Muzaffer Degertekin³

¹Sabanci University, ²Georgia Institute of Technology, ³Yeditepe University Hospital,
{suheylacetin,gozdeunal**,ademir}@sabanciuniv.edu,
anthony.yezzi@ece.gatech.edu, mdegertekin@yeditepe.edu.tr

Abstract. In this paper, we propose a novel tubular structure segmentation method, which is based on an intensity-based tensor that fits to a vessel. Our model is initialized with a single seed point and it is capable of capturing whole vessel tree by an automatic branch detection algorithm. The centerline of the vessel as well as its thickness is extracted. We demonstrated the performance of our algorithm on 3 complex contrast varying tubular structured synthetic datasets for quantitative validation. Additionally, extracted arteries from 10 CTA (Computed Tomography Angiography) volumes are qualitatively evaluated by a cardiologist expert's visual scores.

Keywords: segmentation, CTA, tubular structures, branch detection, vessel trees, coronary arteries, tensor estimation, tractography, tensor

1 Introduction

Delineation of vascular structures is a crucial step in diagnosis, treatment and surgery planning. However, manual segmentation of vascular structures such as blood vessels, coronary arteries or other tube-like structures is an exhaustive task for the experts. As a solution, initially methods such as image enhancement [1, 2], minimal path techniques [3, 4] were proposed. An extensive treatment of these methods can be found in [5] and [6] surveys. Recently, multi-hypotheses tracking techniques have been one of the most popular methods in the literature [7, 8].

Another category for vessel extraction is based on an improvement on minimal path techniques. Li and Yezzi [9] proposed an innovative approach by modeling the vessel as a 4D curve (a radius function and a centerline), thus the centerline is extracted without any additional effort. This method does not take into account the vessel orientation. To improve this method, Mohan et. al. [10] associated to the 4D path an anisotropic potential related to Finsler metric, where they considered the vessel orientation. Optimally Oriented Flux (OOF) based approaches, which take into account the vessel orientation are presented by [11] and [12]. To propagate faster along the vessel, Benmansaur et. al. [12] suggest an anisotropic metric, which is based on the OOF descriptor that have a scalar function and orientation.

** This work was supported by Turkish Scientific and Technical Research Council (TUBITAK), Project No: 108E162 and 108E126.

In this paper, we design a novel tubular structure segmentation method (Section 2.1), which constructs an intensity-based tensor that fits to a vessel, which is inspired from diffusion tensor image (DTI) modeling. The anisotropic tensor inside the vessel drives the segmentation analogously to a tractography approach in DTI. The advantage of our approach over existing methods is that our model is capable of finding the vessel orientation and its thickness at the same time. In our method, the vessel extraction is initialized with a single seed point and entire vessel tree (Section 2.2) can be captured by an automatic branch detection algorithm (Section 2.3). We also develop an unsupervised branch clustering method, which helps to find multiple branchings on complex tree structures.

2 Methods

We propose an intensity based tensor model, which is well suited for tubular structures as vessels. Although similar to Li and Yezzi’s idea [9], a 4D curve representation is used, our contribution is to involve potential measurements from intensity at various spatial directions and use them in a linear least squares tensor fitting to estimate a rank 2 tensor.

2.1 Intensity based tensor fitting

Our vessel model is constructed as follows:

$$\hat{C}(u) = (\mathbf{c}(u), r(u)) \quad , \quad \hat{C} \in \mathbb{R}^4 \quad , \quad u \in [0, L] \quad (1)$$

where $\mathbf{c}(u)$ represents the location on a vessel centerline in \mathbb{R}^3 , $r(u) \in [r_{min}, r_{max}]$ represents the radius of a sphere centered at $\mathbf{c}(u)$, L is the length of the vessel. A sphere can be defined at a point $\mathbf{x}_s \in \mathbb{R}^3$, which is a centerline coordinate as $sph = (\mathbf{x}_s, r)$. A cylinder along each sampled orientation is defined as $cyl = (disk(\mathbf{x}_d, r, \mathbf{v}), h)$ where \mathbf{x}_d is defined as a point in \mathbb{R}^2 , \mathbf{v} is an orientation vector in \mathbb{R}^3 and h ($h=3r$) is defined as the height of the cylinder. The orientation vectors are specified by dense sampling over a unit sphere \mathbb{S}^2 . Each potential measurement M_i , is an image based feature which is modeled according to the intensity properties of the vessel. The potential is based on a difference between the intensity mean μ_{Ω_1} of the sphere, Ω_1 and intensity mean μ_{Ω_2} of the the region, Ω_2 , where $\Omega_1 = sph$ and $\Omega_2 = cyl - sph$. The sketch in Figure 1 illustrates the measurement model, a sphere and the cylinders around the sphere in different orientations. The Figure 1(a) depicts three different orientations $\mathbf{g}_1, \mathbf{g}_2, \mathbf{g}_3$ and the cylinders located along these orientations. The regions Ω_1 and Ω_2 are shown in Figure 1(b) and unit orientations on \mathbb{S}^2 are illustrated in Figure 1(c). Formally, M_i is expressed as follows:

$$M_i = (\mu_{\Omega_1} - \mu_{\Omega_2})^2 \quad (2)$$

and measurement orientations are defined as a matrix: $\mathbf{g} = [\mathbf{g}_1 \quad \mathbf{g}_2 \quad \cdots \quad \mathbf{g}_m]$ where $\mathbf{g}_i = [g_{ix} \quad g_{iy} \quad g_{iz}]^T$ is the column vector for each measurement orientation and m is the number of orientations on \mathbb{S}^2 . M_i can be modelled as $M_i = \mathbf{g}_i^T \mathbf{D} \mathbf{g}_i$ using a 3×3 tensor:

$$\mathbf{D} = \begin{bmatrix} d_{xx} & d_{xy} & d_{xz} \\ d_{yx} & d_{yy} & d_{yz} \\ d_{zx} & d_{zy} & d_{zz} \end{bmatrix}. \quad (3)$$

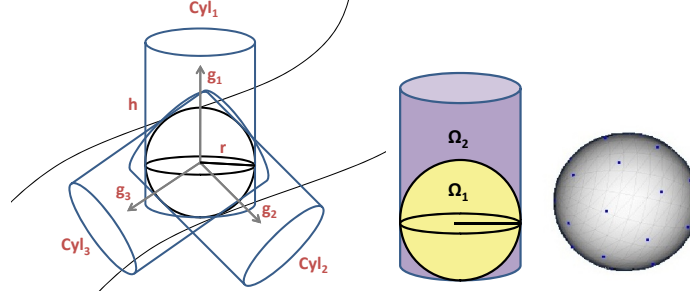


Fig. 1. Illustration of the (a) measurements model (left); (b) cylinder model (middle); (c) orientations on the sphere* (right).

*Figure from BioImage Suite Tool, Yale University School of Medicine

After the measurements $\mathbf{M}_{m \times 1}$ are calculated for all orientations, the tensor \mathbf{D} is calculated by a least squares fitting as explained next. To solve for \mathbf{D} from $M_i = \mathbf{g}_i^T \mathbf{D} \mathbf{g}_i$ equation, we can simply stack the components of \mathbf{D} since \mathbf{D} is a symmetric matrix, as $\mathbf{d} = [d_{xx} \ d_{yy} \ d_{zz} \ d_{xy} \ d_{xz} \ d_{yz}]^T$ and reconstruct the equation as

$$M_i = \mathbf{H}_i \mathbf{d}, \quad (4)$$

where \mathbf{H}_i is the i^{th} row of a matrix:

$$\mathbf{H} = \begin{bmatrix} g_{1x}^2 & g_{1y}^2 & g_{1z}^2 & 2g_{1x}g_{1y} & 2g_{1x}g_{1z} & 2g_{1y}g_{1z} \\ \vdots & \vdots & \vdots & \vdots & \vdots & \vdots \\ g_{mx}^2 & g_{my}^2 & g_{mz}^2 & 2g_{mx}g_{my} & 2g_{mx}g_{mz} & 2g_{my}g_{mz} \end{bmatrix} \quad (5)$$

In matrix form, Eq. 4 becomes $\mathbf{M} = \mathbf{H} \mathbf{d}$. Linear least squares fitting is applied to solve for \mathbf{d} as $\mathbf{d} = (\mathbf{H}^T \mathbf{H})^{-1} \mathbf{H}^T \mathbf{M}$.

Vessel Lumen Thickness Estimation: To estimate the tensor which describes the direction of the vessel and the radius of the sphere, the tensor \mathbf{D}^r is calculated $\forall r \in [r_{min}, r_{max}]$ at a point inside the vessel. When the diameter of the sphere is below or above the vessel lumen thickness, the measurements M_i become lower. The M_i thus becomes largest with the sphere which is tangent to the vessel and, hence the radius of the sphere is detected as:

$$\hat{r} = \underset{r}{\operatorname{argmax}} \|\mathbf{D}^r\|, \forall r \in [r_{min}, r_{max}] \quad (6)$$

where $\|\cdot\|$ denotes 2-norm of the matrix \mathbf{D}^r . That is, the norm of the tensor in Eq. 6 happens to be largest when the sphere fits to the vessel boundary. Estimated tensor \mathbf{D} is equal to $\mathbf{D}^{\hat{r}}$. After the tensor \mathbf{D} is computed, it is decomposed into its eigenvalues and eigenvectors using SVD(Singular Value Decomposition): $\mathbf{D} = \mathbf{V} \boldsymbol{\lambda} \mathbf{V}^T$, where $\lambda_1, \lambda_2, \lambda_3$ are the eigenvalues and $\mathbf{V} = [\mathbf{v}_1, \mathbf{v}_2, \mathbf{v}_3]$ are the eigenvectors of the tensor. \mathbf{v}_3 represents the smallest eigenvector of the tensor. In Figure 2(a), a synthetic Y-shaped vessel data [13] at constant thickness is shown. Norm of the tensor is plotted as a function of sphere radius in Figure 2(b). For instance, the norm at radius 3 becomes maximum for a specific voxel chosen from the centerline of the synthetic data.

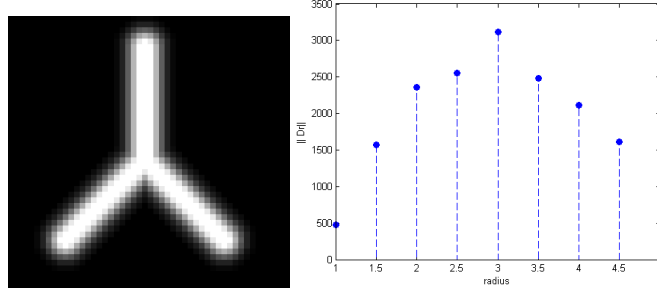


Fig. 2. (a) $60 \times 60 \times 60$ synthetic vessel volume with radius 3; (b) Norm of a tensor for a voxel on the centerline of the synthetic data.

The tensor \mathbf{D} consists of two major eigenvectors, so it becomes a planar ellipsoid as shown in Figure 3. Shape of the tensors on the centerline are more planar and have bigger norm than the others. In addition, when the radius is smaller or larger than the true radius, the norm of the tensor becomes lower. Similarly, since the intensity distribution changes less along the vessel direction, the measurements taken through this direction becomes lower, and this tends to have smallest eigenvector in vessel direction. The smallest eigenvector of the tensor \mathbf{D} thus happens to show ultimately the vessel orientation.

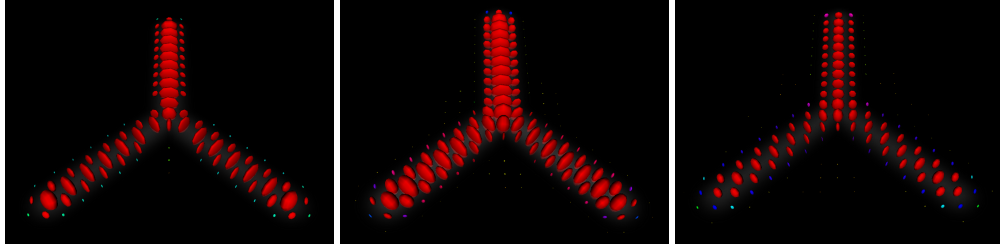


Fig. 3. Estimated tensors are shown for $60 \times 60 \times 60$ synthetic vessel volume; (a) radius is 2 (left); (b) radius is 3 - true radius (middle); (c) radius is 4 (right).

2.2 Vessel tractography

We define a vessel tractography, which traces the centerline of a vessel using the intensity based tensor \mathbf{D} , inspired by the DTI tractography that uses a diffusion tensor. Vessel tractography starts with a user defined initial seed point. The seed point is preferably selected at the center of one of the cross sections of the vessel. The tract, i.e. the 3D centerline, starts to propagate along the positive and negative directions of the eigenvector corresponding to the smallest eigenvalue of the planar tensor. For all spatial coordinates along the tract, the tensor is calculated as explained in Section 2.1. Minor vector of the tensor is obtained and a new tract coordinate $\mathbf{c}(u_n)$ is calculated by adding the \mathbf{v}_3 vector (describes the principal orientation of the vessel which is the smallest eigenvector of the tensor at $\mathbf{c}(u_{n-1})$) to the current coordinate $\mathbf{c}(u_{n-1})$. To avoid tract aberrations, a streamline tractography (SLT) [14] method is preferred. SLT uses the vessel orientation by weighting it with α to compute Euler's method approximation to

the parametrized tract $\mathbf{c}(u)$ as follows:

$$\mathbf{c}(u_n) = \mathbf{c}(u_{n-1}) + \alpha \frac{d\hat{\mathbf{c}}(u)}{du} \rightarrow \mathbf{c}(u_n) \approx \mathbf{c}(u_{n-1}) + \alpha \mathbf{v}_3, \quad (7)$$

where $\mathbf{c}(u = 0)$ is the seed point, and $0 \leq u_n \leq L$, L is the length of the vessel. The tract is computed using a piecewise linear step size in the direction of \mathbf{v}_3 . Tract propagation occurs in both collinear tangent directions approximated by \mathbf{v}_3 .

The tractography algorithm continues till pre-defined convergence criteria are satisfied. First convergence criterion is the mean intensity ratio between the spherical region of the seed and the current coordinate $\mathbf{c}(u_{n-1})$. The sphere centered at the seed point is defined as $sph_1 = (\mathbf{c}_{seed}, r_{seed})$ and sphere at the current coordinate $\mathbf{c}(u_{n-1})$ is $sph_2 = (\mathbf{c}(u_{n-1}), r)$, and the regions are specified as $\Omega_1 = sph_1$ and $\Omega_2 = sph_2$. If the ratio $\beta_1 = \mu_{\Omega_2}/\mu_{\Omega_1}$ is below a given threshold, this implies that the tract reaches the end of the vessel and the tractography stops at this point. Second termination criterion is defined from the ratio $\beta_2 = \mu_{\Omega_3}/\mu_{\Omega_2}$ where $\Omega_3 = sph_3 - sph_2$ and $sph_3 = (\mathbf{c}(u_{n-1}), 2r)$. When $\mathbf{c}(u_{n-1})$ reaches the origin (coronary ostium) or the end of artery, β_2 is assumed to be approximately 1. β_2 is used both to force tract to stop at the end of vessel and to prevent the tract to diverge toward regions around the vessel. In addition, a third criterion, which stops the tract when the radius r at point $\mathbf{c}(u_{n-1})$ reaches to $r = r_{max}$, is used to avoid divergence of the vessel tract to surrounding blob regions.

Centralization: Sometimes a tract or centerline of the vessel can aberrate because of the effects of tensor perturbation. In this case, a centralization procedure should be applied to the tract. First, a multiplanar reconstruction method (MPR) (Eq. 8) is applied at the coordinate $\mathbf{c}(u_{n-1})$ to find a projection slice which has \mathbf{v}_3 as its normal vector. Then, \mathbf{v}_1 and \mathbf{v}_2 define the reconstructed plane. The MPR plane image is defined as

$$I_{prj}(i, j) = I(\mathbf{c}(u_{n-1}) + (i - x_c)\mathbf{v}_1 + (j - y_c)\mathbf{v}_2) \quad (8)$$

where I is the original image to be projected, I_{prj} is the projection image and x_c, y_c are the coordinate centers of the I_{prj} . After the subregion or projected plane around the coordinate through \mathbf{v}_1 and \mathbf{v}_2 is calculated, then an $r \times r$ (the radius is found during tensor fitting) kernel is applied on this plane to find the coordinate which has the maximum brightness. This plane is chosen to be large enough to involve the vessel boundaries and surroundings near the vessel, but not very large to compromise other structures around vessel. Typically, it is chosen as 40×40 in image coordinates. (x', y') represent the coordinates of the maximum brightness point, which is found as:

$$(x', y') = \underset{x, y}{\operatorname{argmax}} \sum_{i, j \in N(x, y)} I_{prj}(i, j), \quad (9)$$

where the neighbourhood function $N(x, y)$ is expressed as $N(x, y) = \{(i, j) | (x - i)^2 + (y - j)^2 \leq r^2\}$. Then the corresponding point in the original image is defined as

$$\mathbf{c}' = \mathbf{c}(u_{n-1}) + (x' - x_c) \frac{\mathbf{v}_1}{2} + (y' - y_c) \frac{\mathbf{v}_2}{2} \quad (10)$$

where \mathbf{c}' is the centralized point, which is the corrected centerline coordinate.

2.3 Branch Detection - Unsupervised Clustering

In order to extend our vessel tractography model to tubular trees, we developed a branch detection method. It is inspired from the Mohan et. al. work [10], which was based on an assumption that vessels have at most two branches to be separated. Their algorithm checks the surrounding regions around the center coordinate $\mathbf{c}(u_{n-1})$ and cluster them in a supervised way via a Kmeans clustering.

We propose an unsupervised clustering method, which is capable of detecting any number of branches. In our method, we assume that the branches of the vessel tree have similar intensity distributions with the main branch. We search the branches on a spherical surface around the current coordinate in a $\frac{5}{3}\pi$ field of view, which avoids the branch candidates that are already processed. Branch candidate coordinates are calculated as:

$$\mathbf{c}_{branch}(i) = \mathbf{c}(u_{n-1}) + 2r\mathbf{g}_i, \quad \mathbf{g}_i \in \mathbf{g} \quad (11)$$

where \mathbf{g} represents orientations on \mathbb{S}^2 as defined in Section 2.1. When the mean of the sphere centered at the branch coordinate has approximately same mean to the sphere centered at the seed, the tensor fitting is applied at that coordinate. Direction of the vectors are used as a cluster classifier in our method. If \mathbf{v}_3 of the tensor of the branch coordinate is not in the direction of the current path, \mathbf{v}_3 and its coordinate is put into a new cluster or to an already existing cluster. (i) When the vector \mathbf{v}_3 is closer to the directions in one of the previously formed clusters, it is inserted into an appropriate cluster with its corresponding coordinate. (ii) When the vector \mathbf{v}_3 has a distinct orientation, a new cluster is constructed and this vector is added with its corresponding coordinate to that cluster. After all orientations are searched, coordinate mean of each cluster is calculated and labelled as a branch coordinate.

3 Results

In this section, we first give a quantitative validation of the performance of our method on synthetic vascular imageries with known ground truth. The datasets are obtained from the work of Hamarneh and Jassi's [15], which simulate volumetric images of vascular trees with varying contrast and generate the corresponding ground truth segmentations. Next, we evaluate our method qualitatively and apply it to extract the coronary arteries from CTA (Computed Tomography Angiography) volumes. For each case, a single seed point is selected from each tree, then entire vessel tree is segmented automatically.

We used 24 unit directions on \mathbb{S}^2 and the radius range is selected between 0.25 and 4 mm in tensor fitting. Additionally, algorithm's termination ratios β_1 and β_2 are chosen as 0.25 and 0.85 respectively for all experiments. We used 4 different quantitative measures as TP (True Positive), FN (False Negative), FP (False Positive) and OM (Overlap Measure) between the estimated vessel map and the ground truth vessel map. Table 1 shows TP, FN, FP and OM rates for the three synthetic vascular datasets. We obtained high TP and OM ratios between 93% and 96%.

Figure 4(a) depicts the extracted centerline of the vascular synthetic data. The user selects a single seed, which is shown with a yellow sphere, from one of

Table 1. Segmentation results of our method on contrast varying synthetic vascular images.

Rate (%)	Data 1	Data 2	Data 3
TP	94.30	94.77	96.13
FN	5.7	5.23	3.87
FP	8.45	4.88	4.76
OM	93.03	93.76	95.70

Table 2. Visual scores of our method on 10 CTA datasets from Pt 1 to Pt 10.

	Pt 1	Pt 2	Pt 3	Pt 4	Pt 5	Pt 6	Pt 7	Pt 8	Pt 9	Pt 10
RCA	5	5	5	5	5	5	5	4	5	5
LM	5	5	5	5	5	5	5	5	4.5	5
LAD	5	5	5	5	4.5	4.5	5	4	4.5	5
LCX	4	5	5	5	5	4.5	5	4	5	5

the branches. Then, the entire tree is extracted automatically by our method. The branch coordinates which are found during the execution of our algorithm is shown by red spheres. Extracted vessel tree (with surface) is shown in Figure 4(b).

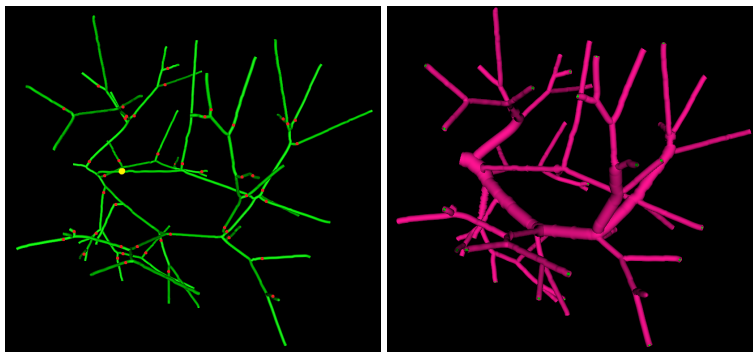


Fig. 4. Extracted vessel tree of the $101 \times 101 \times 101$ synthetic vascular dataset; (a) Centerline is depicted by green, branching points by red and seed by yellow; (b) Surface of the segmentation is shown by pink.

Next, we used our method to extract the coronary arteries from 10 CTA volumes as shown on Table 2. For a qualitative evaluation; a cardiologist expert gave scores (0-5) to RCA (Right Coronary Artery), LM (Left Main), LAD (Left Anterior Descending) and LCX (Left Circumflex Artery) by considering the length, thickness and centerline of each artery. We obtained high scores for each dataset. Figure 5 shows extracted arteries for patient 2, patient 5 and patient 8.

4 Discussions

In this work, we proposed a method for extracting vessel trees using a novel intensity-based tractography idea. We also proposed an automatic branch detection algorithm, which is capable of finding any number of branches in vascular structures. We demonstrated the performance of our method by quantitative analysis of synthetic volumes and by qualitative analysis of extraction of arteries from

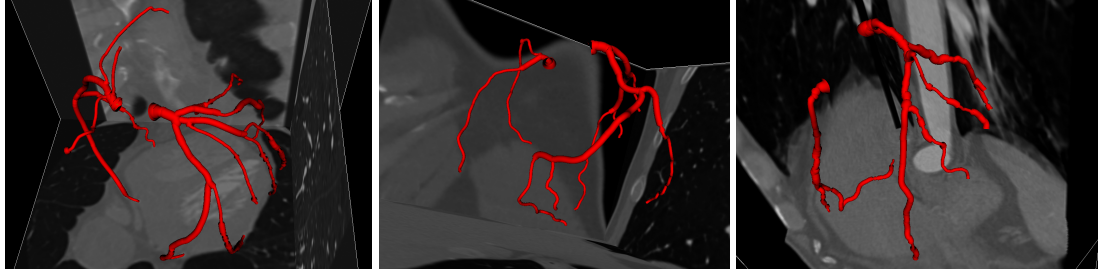


Fig. 5. Visualization of extracted arteries from 2nd (left), 5th (middle) and 8th (right) patient volumes.

CTA imagery. Currently, we are testing our algorithm on Rotterdam Coronary Artery database [16], which provides a quantitative evaluation framework where several algorithms can be compared with the others.

References

1. Frangi, R., Niessen, W., Vincken, K., Viergever, M.: Multiscale vessel enhancement filtering. (1998) 130–137
2. Krissian, K.: Flux-based anisotropic diffusion applied to enhancement of 3-d angiogram. *IEEE Trans. Med. Imaging* **21**(11) (2002) 1440–1442
3. Deschamps, T., Cohen, L.D.: Fast extraction of minimal paths in 3d images and applications to virtual endoscopy. *Med. Imag. Anal.* **5**(4) (2001) 281 – 299
4. Cohen, L., Kimmel, R.: Global minimum for active contour models: A minimal path approach. *International Journal of Computer Vision* **24** (1997) 57–78
5. Kirbas, C., Quek, F.: A review of vessel extraction techniques and algorithms. *ACM Comput. Surv.* **36** (2004) 81–121
6. Lesage, D., Angelini, E.D., Bloch, I., Funka-Lea, G.: A review of 3D vessel lumen segmentation techniques. *Med. Imag. Anal.* **13**(6) (2009) 819–845
7. Lesage, D., Angelini, E.D., Bloch, I., Funka-Lea, G.: Bayesian maximal paths for coronary artery segmentation from 3d ct angiograms. (2009) 222–229
8. Friman, O., Hindennach, M., Kühnel, C., Peitgen, H.O.: Multiple hypothesis template tracking of small 3D vessel structures. *Med. Imag. Anal.* **14**(2) (2010) 160–171
9. Li, H., Yezzi, A.J.: Vessels as 4-d curves: Global minimal 4-d paths to extract 3-d tubular surfaces and centerlines. *IEEE Trans. Med. Imaging* **26**(9) (2007) 1213–1223
10. Mohan, V., Sundaramoorthi, G., Tannenbaum, A.: Tubular surface segmentation for extracting anatomical structures from medical imagery. (*IEEE Trans. Med. Imag.*)
11. Law, M.W., Chung, A.C.: Three dimensional curvilinear structure detection using optimally oriented flux. In: *Pro. Conference Computer Vision.* (2008)
12. Benmansour, F., Cohen, L.D.: Tubular anisotropy segmentation. In: *Pro. Conference Scale Space and Variational Methods in Computer Vision.* (2009)
13. Krissian, K., Malandain, G.: Synthetical test images for vascular segmentation algorithms. (<http://lmi.bwh.harvard.edu/research/vascular/SyntheticVessels/SyntheticVesselImages.html>)
14. Basser, P.J., Pajevic, S., Pierpaoli, C., Duda, J., Aldroubi, A.: In vivo fiber tractography using DT-MRI data. *Magnetic resonance in medicine* **44**(4) (2000) 625–632
15. Hamarneh, G., Jassi, P.: Vascusynth: Simulating vascular trees for generating volumetric image data with ground-truth segmentation and tree analysis. *Computerized Medical Imaging and Graphics* **34**(8) (2010) 605 – 616
16. Schaap, M., Metz, C., Walsum, T.V., Niessen, W.: Rotterdam coronary artery algorithm evaluation framework. (<http://coronary.bigr.nl/>)